Inorg. Chem. **2005**, *44*, 4451–4453

High-Frequency and -Field EPR Investigation of a Manganese(III) N-Confused Porphyrin Complex, [Mn(NCTPP)(py)$_2$]

John D. Harvey,[†] Christopher J. Ziegler,[†] Joshua Telser,[‡] Andrew Ozarowski,[§] and J. Krzystek*[,§]

Department of Chemistry, University of Akron, Akron, Ohio 44325, Chemistry Program, Roosevelt University, Chicago, Illinois 60605, National High Magnetic Field Laboratory, Florida State University, Tallahassee, Florida 32310

Received May 2, 2005

We report the first high-frequency and -field electron paramagnetic resonance (HFEPR) study of a Mn(III) N-confused porphyrin (NCP) complex (NCP is also known as inverted porphyrin or 2-aza-21-carbaporphyrin). We have found a striking variation in the electronic properties of the $S = 2$ Mn(III) ion coordinated by NCP compared to other Mn(III) porphyrinoid complexes. Thus, inversion of a single pyrrole ring greatly changes the equatorial ligand field exerted and leads to large magnitudes of both the axial and rhombic zero-field splitting [respectively, $D = -3.084(3)$ cm^{-1}, $E = -0.608(3)$ cm^{-1}], which are unprecedented in other Mn(III) porphyrinoids.

Among the isomers and analogues of porphyrin, NCP (also known as inverted porphyrin or 2-aza-21-carbaporphyrin)[1] is unique both in its striking similarities and in its differences with normal porphyrins.[2,3] Although the structure of NCP (Chart 1) is nearly identical to that of its parent porphyrin, its physical and chemical properties differ significantly, as observed in the tautomeric behavior[4] and metallation chemistry[5] of NCP. In particular, the trianionic form of NCP shares some similarities with corrole and corrolazine, which have been shown to stabilize high-valent oxidation states in metal complexes.[6,7] Recently, significant progress has been made toward the synthesis of NCP metal compounds and biomimetic models.[8,9] Among these, we prepared the complex [Mn(III)(NCTPP)(py)$_2$] (**1**, Chart 1) by use of $Mn_2(CO)_{10}$ as the metallating reagent,[10] followed by air oxidation in the presence of pyridine. Thus far, metallo-NCP complexes have not been extensively characterized by spectroscopic methods, particularly by EPR spectroscopy, which is generally very useful for probing the electronic structure of paramagnetic metalloporphyrins.[11] In particular, Mn(III) porphyrins have proven to be very amenable to high-frequency and -field electron paramagnetic resonance (HFEPR) studies. The sizable zero-field splitting (zfs) of the non-Kramers Mn(III) ion ($S = 2$) makes these complexes "EPR-silent" at conventional frequencies and fields but is an advantage for HFEPR experiments. Thus, the information on zfs obtained from several Mn(III) complexes of porphyrins[12,13] and related molecules such as porphyrazines,[14] corroles,[15] and corrolazines[16] has served to characterize the relation between geometric and electronic structure of these complexes. To our best knowledge, however, no HFEPR experiment has been reported on an N-confused porphyrin Mn(III) complex. It was thus of interest to use the Mn(III) ion as a probe

Chart 1. Structures of Internally Protonated Freebase N-Confused Porphyrin (left) and [Mn(NCTPP)(py)$_2$] Complex (right)[8]

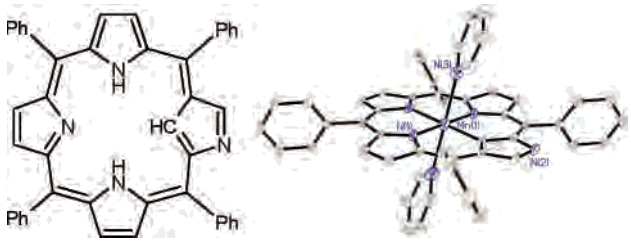

* To whom correspondence should be addressed. E-mail: krzystek@fsu.edu.
† University of Akron.
‡ Roosevelt University.
§ Florida State University.

(1) Abbreviations used: EPR, electron paramagnetic resonance; HFEPR, high-frequency and -field EPR; AOM, angular overlap model; bpea, *N*,*N*′-bis(2-pyridylmethyl)ethylamine; dbm, anion of 1,3-diphenyl-1,3-propanedione (dibenzoylmethane); DEHMC, trianion of 8,12-diethyl-2,3,7,13,17,18-hexamethylcorrole; DFT, density functional theory; NCP, N-confused porphyrin; NCTPP, trianion of 5,10,15,20-tetraphenyl-N-confused porphyrin; py, pyridine; terpy, 2,2′:6′,2″-terpyridine; zfs, zero-field splitting.

(2) Furuta, H.; Asano, T.; Ogawa, T. *J. Am. Chem. Soc.* **1994**, *116*, 767−768.
(3) Chmielewski, P. J.; Latos-Grażyñski, L.; Rachlewicz, K.; Głowiak, T. *Angew. Chem., Int. Ed. Engl.* **1994**, *33*, 779−781.
(4) Furuta, H.; Ishizuka, T.; Osuka, A.; Dejima, H.; Nakagawa, H.; Ishikawa, Y. *J. Am. Chem. Soc.* **2001**, *123*, 6207−6208.
(5) Harvey, J. D.; Ziegler, C. J. *Coord. Chem. Rev.* **2003**, *247*, 1−19.
(6) Gross, Z.; Golubkov, G.; Simkhovich, L. *Angew. Chem., Int. Ed.* **2000**, *39*, 4045−4047.
(7) Mandimutsira, B. S.; Ramdhanie, B.; Todd, R. C.; Wang, H.; Zareba, A. A.; Czernuszewicz, R. S.; Goldberg, D. P. *J. Am. Chem. Soc.* **2002**, *124*, 15170−15171.
(8) Harvey, J. D.; Ziegler, C. J. *Chem. Commun.* **2003**, 2890−2891.
(9) Harvey, J. D.; Ziegler, C. J. *Chem. Commun.* **2004**, 1666−1667.
(10) Buchler, J. W. In *The Porphyrins*; Dolphin, D., Ed.; Academic Press: New York, 1978; Vol. 1, pp 389−481.
(11) Walker, F. A. In *The Porphyrin Handbook*; Kadish, K. M., Smith, K. M., Guillard, R., Eds.; Academic Press: New York, 2000; Vol. 5, pp 81−183.
(12) Krzystek, J.; Telser, J.; Pardi, L. A.; Goldberg, D. P.; Hoffman, B. M.; Brunel, L.-C. *Inorg. Chem.* **1999**, *38*, 6121−6129.
(13) Krzystek, J.; Pardi, L. A.; Brunel, L.-C.; Goldberg, D. P.; Hoffman, B. M.; Licoccia, S.; Telser, J. *Spectrochim. Acta A* **2002**, *58*, 1113−1127.

10.1021/ic0506759 CCC: $30.25
Published on Web 05/21/2005

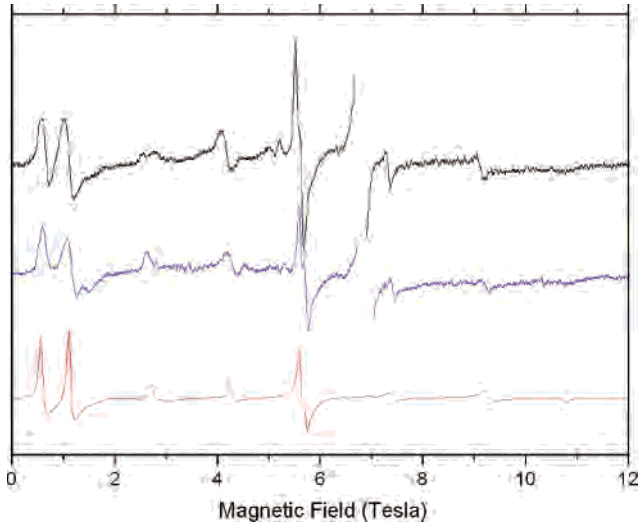

Figure 1. (Top) Experimental HFEPR spectra of polycrystalline complex **1** (black trace) at 192 GHz and 10 K and of the same complex at 150 mM in pyridine solution under the same conditions (blue trace). The red trace represents a powder-pattern simulation using the following set of spin Hamiltonian parameters: $S = 2$, $D = -3.08$ cm^{-1}, $E = -0.61$ cm^{-1}, $g_{iso} = 2.00$. A narrow, high-amplitude $g = 2.00$ signal from trace Mn(II) impurity has been cut off in the experimental spectra and is not reproduced in the simulation.

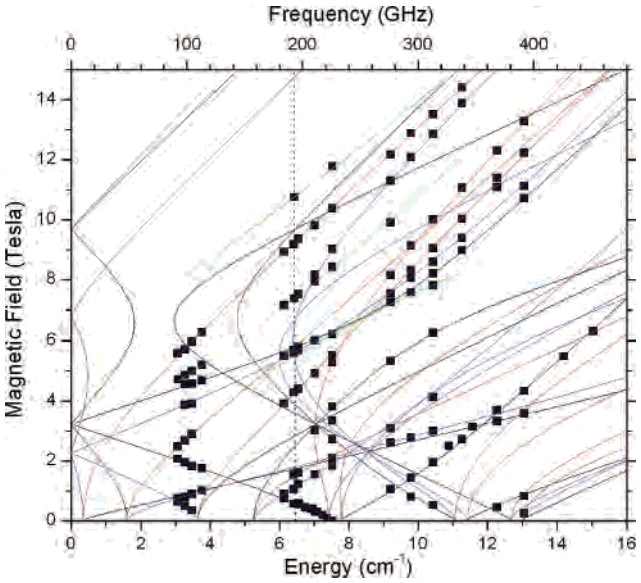

Figure 2. Resonance field vs quantum energy (or frequency) dependence of HFEPR signals in polycrystalline complex **1** at 10 K. The squares are experimental points; the curves were simulated using the best-fit spin Hamiltonian parameters as reported in the text. Red lines, turning points with $B_0 \| x$; blue lines, turning points with $B_0 \| y$; black lines, turning points with $B_0 \| z$; green lines, off-axis turning points. Transitions shown in Figure 1 can be identified using the dotted line drawn parallel to the y axis at 192 GHz (6.4 cm^{-1}).

sensing its environment in the modified cavity offered by N-confused porphyrins.

Complex **1** was investigated using HFEPR spectrometers of the Millimeter and Sub-millimeter Wave Spectroscopy Facility[17] and the EMR Facility[18] at the National High Magnetic Field Laboratory. The complex was measured as a polycrystalline solid "as is". No obvious effects of torquing in the applied field were observed. A typical low-temperature HFEPR spectrum is shown in Figure 1, top (black trace). To ascertain that the spin Hamiltonian parameters extracted from the spectra represent intrinsic properties of the complex and do not result from, e.g., crystal-packing phenomena, we also performed an experiment on the complex in pyridine frozen solution at a concentration of 150 mM. The resulting spectra (Figure 1, blue trace) were practically identical to those of the solid at any given frequency. The spin Hamiltonian parameters that reproduced them through simulations (red trace) were thus the same for the polycrystalline samples and the frozen solution within the accuracy of the method.

Although the agreement between the experiments and simulations can be considered very good, no further attempt was made to optimize the spin Hamiltonian parameters from single-frequency spectra. Instead, we performed multifrequency experiments on the polycrystalline sample using tunable sources and collected a two-dimensional data array of resonance fields vs quantum energies. This data set is presented as squares in Figure 2. Spin Hamiltonian parameters were obtained by a simultaneous fit to *all* experimental points. This procedure, described in more detail elsewhere,[19] led to the following set of spin Hamiltonian parameters defined as usual by[20]

$$\mathcal{H} = \beta B \cdot \mathbf{g} \cdot S + D[S_z^2 - S(S+1)/3] + E(S_x^2 - S_y^2) + \text{(fourth-order zfs terms)} \quad (1)$$

where $S = 2$, $D = -3.084(3)$ cm^{-1}, $E = -0.608(3)$ cm^{-1}, $g_x = 2.000(2)$, $g_y = 2.000(3)$, and $g_z = 2.006(4)$. The data quality was sufficiently high for the fitting software to explore the contribution of fourth-order zfs parameters; however, these parameters are zero within statistical error.

The first conclusion from the EPR spectra is that the ground state of the complex is unequivocally described as a spin quintet ($S = 2$). This should be mentioned in the context of previous work on **1**,[8] where susceptibility measurements characterized the ground spin state of the complex as intermediate ($S = 1$). A comparison of the zfs parameters of complex **1** with those typical for porphyrinic Mn(III) complexes immediately shows the effect of reduced symmetry of the ligand appearing as a significant rhombicity of the zfs tensor. Whereas all known Mn(III) porphyrins (and porphyrazines) are characterized by a strictly axial zfs tensor ($E = 0$) and Mn(III) corroles (and corrolazines) exhibit only

(14) Goldberg, D. P.; Telser, J.; Krzystek, J.; Montalban, A. G.; Brunel, L.-C.; Barrett, A. G. M.; Hoffman, B. M. *J. Am. Chem. Soc.* **1997**, *119*, 8722−8723.
(15) Krzystek, J.; Telser, J.; Hoffman, B. M.; Brunel, L.-C.; Licoccia, S. *J. Am. Chem. Soc.* **2001**, *123*, 7890−7897.
(16) Lansky, D. E.; Mandimutsira, B.; Ramdhanie, B.; Clausen, M.; Penner-Hahn, J.; Zvyagin, S. A.; Telser, J.; Krzystek, J.; Zhang, R.; Ou, Z.; Kadish, K. M.; Zhakarov, L.; Rheingold, A. L.; Goldberg, D. P. *Inorg. Chem.* **2005**, in press.
(17) Zvyagin, S. A.; Krzystek, J.; van Loosdrecht, P. H. M.; Dhalenne, G.; Revcolevschi, A. *Physica B* **2004**, *346*−*347*, 1−5.
(18) Hassan, A. K.; Pardi, L. A.; Krzystek, J.; Sienkiewicz, A.; Goy, P.; Rohrer, M.; Brunel, L.-C. *J. Magn. Reson.* **2000**, *142*, 300−312.
(19) Aromí, G.; Telser, J.; Ozarowski, A.; Brunel, L. C.; Krzystek, J. *Inorg. Chem.* **2005**, *44*, 187−196.
(20) Abragam, A.; Bleaney, B. *Electron Paramagnetic Resonance of Transition Ions*; Dover Publications: New York, 1986.

a very slight degree of rhombicity ($E/D < 0.01$),[15] complex **1** displays a high ratio of $E/D = 0.20$ (the maximum possible E/D value is 0.33, as follows from eq 1). This ratio does not result from a low magnitude of D; indeed, $|D|$ is at the high limit observed for Mn(III) tetrapyrroles.[21] The most relevant among these is [Mn(DEHMC)(py)$_2$], for which $D = -2.78$ cm^{-1} ($E = 0.03$ cm^{-1}).[15] This Mn(III) corrole complex has the same axial ligands as **1**; thus, the difference between the two is a direct measure of the effect of the NCP macrocycle versus the corrole. Specifically, the larger magnitude of D for **1** is a consequence of the greater strength of the equatorial ligand field produced by the $(N_2C)^{3-}$ donor set of NCP relative to the $(N_3)^{3-}$ of corrole. In addition to increasing the overall equatorial ligand field, the C donor also provides an asymmetry that leads to the very large rhombic term in zfs.

The zfs tensor of complex **1** can also be compared to those found in low-symmetry, six-coordinate complexes of Mn(III) of general formula [Mn(L)X$_3$], where L = terpy, bpea; X = azide, fluoride.[22,23] The magnitudes of both D and E for the [Mn(L)X$_3$] complexes are quite close to that for **1**, which suggests that, even though the donor set and geometry of the [Mn(L)X$_3$] complexes are seemingly unrelated to that of **1**, their net effect on the electronic structure of Mn(III) is similar. Qualitatively, the N_3 donors of NCTPP are equivalent to those of terpy, whereas the C donor of NCTPP is as different from the other equatorial N_3 donors of NCTPP as fluoride or azide is from the terpy N_3 donors, leading in both cases to the largely rhombic zfs that is absent in porphyrins and related complexes with equatorial N_4 donor sets. Comparison of the axial ligands is difficult, as the [Mn(L)X$_3$] complexes have π-cylindrical axial ligands (F^-, N_3^-), whereas asymmetric π-bonding by the py ligands of **1** is potentially complicated, as discussed previously for [Mn(dbm)$_2$py$_2$]$^+$.[19] Evidently, the difference in ligand fields between the axial and equatorial donors in **1** must be similar to that in the [Mn(L)X$_3$] complexes.

Computational methods, such as DFT, have been widely applied to metalloporphyrins.[24−26] Such studies as applied to complex **1** are in progress but beyond the scope of this Communication. At present, we apply more qualitative methods, namely, ligand-field theory, such as some of us have used previously.[12] We take as a starting point the ligand-field parameters estimated earlier for Mn(III) porphyrins[12] (in cm^{-1}), i.e., $Dq \approx 2700$, $Ds \approx 2800$, $Dt \approx 2400$ (parameters as defined by Ballhausen[27]), where Dq is a cubic splitting and Ds and Dt describe tetragonal distortion, and modify them to account for an increased equatorial field. This effect is achieved here by reducing the tetragonal parameter, Dt, which leads to an increase in the magnitude of the axial zfs, D. A large rhombic term, Dr,[28] necessarily absent in the axial porphyrins, is then included. Use of the full d^4 basis set and the set of electronic parameters (in cm^{-1}) $Dq = 2700$, $Ds = 2800$, $Dt = 1800$, $Dr = 1800$; Racah parameters,[29] $B = 700$ (∼75% of the free-ion value, which accounts for the high covalency of **1**), $C = 3000$ (∼4.3B), and spin−orbit coupling $\zeta = 300$ (∼85% of the free-ion value)[29] gives a ground-state spin quintet with $D = -3.0$, $|E| = 0.6$ cm^{-1}. Furthermore, this set of electronic parameters can roughly describe the range of zfs in Mn(III) porphyrinic complexes. For example, the set given above, except with $Dr = 0$, gives $D = -3.00$ cm^{-1} (an "axial" NCP). The same set, but with $Dr = 0$ and $Dt = 2400$, gives $D = -2.67$ cm^{-1}, similar to what is observed for Mn(III) complexes with the trianionic corroles.[15,30] Introducing larger Racah parameters (e.g., $B = 800$), representative for the lower covalency of a dianionic macrocycle, yields $D = -2.16$ cm^{-1}, typical for Mn(III) complexes of regular porphyrins.[13]

We emphasize that, although internally consistent, these ligand-field parameters are highly approximate, especially given the lack of corroboration with identifiable ligand-field (d−d) transitions, in contrast to complexes with simpler, unconjugated, more innocent ligands, such as $[Mn(H_2O)_6]^{3+}$, where such transitions are visible, and an AOM analysis could be performed.[31] Nevertheless, our analysis indicates the extremely large field generated by the equatorial carbanion, so that it is possible that the principal zfs direction is along the N−Mn−C vector, rather than normal to the macrocycle plane, as would be the case for typical metalloporphyrins.

Overall, the HFEPR results for complex **1** show rather astonishing changes in the properties of Mn(III) compared to regular Mn(III) porphyrinic complexes. Most strikingly, the swapping of just two atoms, that is, one equatorial N donor with a C donor in the porphyrin backbone, results in a significant variation in the zfs tensor compared to that of normal Mn(III) porphyrin—a consequence of a much greater effect on the electronic structure of the Mn(III) ion than any change in a porphyrinic macrocycle observed to date. Inversion of a single pyrrole generates a very strong equatorial ligand field effect, producing a large D and rhombic zfs as yet unobserved in other Mn(III) porphyrinoids.

Acknowledgment. NHMFL is funded by the NSF through Cooperative Agreement DMR 0084173 and the State of Florida. The W. M. Keck Foundation funded the 25-T resistive magnet. We thank Drs. Høgni Weihe and Jesper Bendix from the University of Copenhagen for the programs SIM and LIGFIELD, respectively.

IC0506759

(21) Krzystek, J.; Telser, J. *J. Magn. Reson.* **2003**, *162*, 454−465.
(22) Limburg, J.; Vrettos, J. S.; Crabtree, R. H.; Brudvig, G. W.; de Paula, J. C.; Hassan, A.; Barra, A.-L.; Duboc-Toia, C.; Collomb, M.-N. *Inorg. Chem.* **2001**, *40*, 1698−1703.
(23) Mantel, C.; Hassan, A. K.; Pécaut, J.; Deronzier, A.; Collomb, M.-N.; Duboc-Toia, C. *J. Am. Chem. Soc.* **2003**, *125*, 12337−12344.
(24) Conradie, J.; Swarts, J. C.; Ghosh, A. *J. Phys. Chem. B* **2004**, *108*, 452−456.
(25) Van Lenthe, E.; Van der Avoird, A.; Hagen, W. R.; Reijerse, E. J. *J. Phys. Chem. A* **2000**, *104*, 2070−2077.
(26) Ghosh, A.; Wondimagegn, T.; Parusel, A. B. J. *J. Am. Chem. Soc.* **2000**, *122*, 5100−5104.
(27) Ballhausen, C. J. *Introduction to Ligand Field Theory*; McGraw-Hill: New York, 1962; pp 99−103.
(28) Defined as: $\langle d_{\pm1}|\boldsymbol{V}_{rhombic}|d_{\mp1}\rangle = Dr$, $\langle d_{\pm2,0}|\boldsymbol{V}_{rhombic}|d_{0,\pm2}\rangle = (2/3)^{1/2}Dr$.
(29) Figgis, B. N.; Hitchman, M. A. *Ligand Field Theory and Its Applications*; Wiley-VCH: New York, 2000.
(30) Bendix, J.; Gray, H. B.; Golubkhov, G.; Gross, Z. *Chem. Commun.* **2000**, 1957−1958.
(31) Tregenna-Piggott, P. L. W.; Weihe, H.; Barra, A.-L. *Inorg. Chem.* **2003**, *42*, 8504−8508.